CHIN. PHYS. LETT. Vol. 38, No. 1 (2021) 010501

Managing Quantum Heat Transfer in a Nonequilibrium Qubit-Phonon Hybrid System with Coherent Phonon States

Chen Wang(王晨)[1*], Lu-Qin Wang(王鲁钦)[2], and Jie Ren(任捷)[2*]

[1]*Department of Physics, Zhejiang Normal University, Jinhua 321004, China*
[2]*Center for Phononics and Thermal Energy Science, China-EU Joint Center for Nanophononics, Shanghai Key Laboratory of Special Artificial Microstructure Materials and Technology, School of Physics Sciences and Engineering, Tongji University, Shanghai 200092, China*

(Received 9 October 2020; accepted 9 November 2020; published online 6 January 2021)

We investigate quantum heat transfer in a nonequilibrium qubit-phonon hybrid open system, dissipated by external bosonic thermal reservoirs. By applying coherent phonon states embedded in the dressed quantum master equation, we are capable of dealing with arbitrary qubit-phonon coupling strength. It is counterintuitively found that the effect of negative differential thermal conductance is absent at strong qubit-phonon hybridization, but becomes profound at weak qubit-phonon coupling regime. The underlying mechanism of decreasing heat flux by increasing the temperature bias relies on the unidirectional transitions from the up-spin displaced coherent phonon states to the down-spin counterparts, which seriously freezes the qubit and prevents the system from completing a thermodynamic cycle. Finally, the effects of perfect thermal rectification and giant heat amplification are unraveled, thanks to the effect of negative differential thermal conductance. These results of the nonequilibrium qubit-phonon open system would have potential implications in smart energy control and functional design of phononic hybrid quantum devices.

DOI: 10.1088/0256-307X/38/1/010501

The tremendous progress of quantum engineering spurs on the generation of hybrid quantum systems (HQSs), which establish multi-tasking platforms for the practical realization in versatile areas, ranging from quantum optics, quantum information science to atomic physics.[1−3] HQSs are typically composed of two or more quantum components, with each owning distinct physical functionality, e.g., spin storing long-lived memory and photon transmitting high-quality information via the spin-photon interface.[4−9] The main advantage of such quantum hybridization is that HQSs overcome individual limitations, and probably make the universal applications.

The representative spin-photon hybrid system is the circuit quantum electrodynamics (cQED) platform, which is generally composed by a superconducting qubit coupled to the on-chip microwave resonator.[3−5] The cQED is theoretically modeled as the Jaynes–Cummings model with weak qubit-photon hybrid interaction[4] and the quantum Rabi model at strong hybrid coupling,[6] respectively. It has been extensively applied to investigate coherent control of quantum photon transport,[9] quantum correlation enhancement out-of-equilibrium,[10] and quantum network communication.[11,12]

As an analogy of photons, quantum information processing[13−17] and quantum logical operation[18,19] have also be widely conducted based on the qubit-phonon hybridization, which typically consists of one two-level qubit mechanically interacting with a phonon mode, which can be realized by single electronic qubit coupled to the nanomechanical resonator[13] or the acoustic resonator,[19] and one quantum dot embedded within a nanowire.[15] If the two-level qubit is replaced by the qubits ensemble, the cooperative effects can be dynamically observed, ranging from the fast phonon dynamics,[20] superradiant lasing[21] to ground state cooling.[22]

Quantum energy flow, which is tightly related with quantum information science, is considered as the key characteristic to detect the nonequilibrium behavior of open quantum systems.[23−26] In particular, the heat transfer has been extensively studied within phononics,[27] e.g., anharmonic phononic lattices.[28−30] While for the phononic HQSs, the vibration mode mostly plays the assistant role to enhance the electron transfer.[31−37] Hence, considering the successful applications of qubit-phonon hybridization in the quantum information science and nonequilibrium effects, we are motivated to exploring

Supported by the National Natural Science Foundation of China (Grant No. 11704093), the Opening Project of Shanghai Key Laboratory of Special Artificial Microstructure Materials and Technology, the National Natural Science Foundation of China (Grant Nos. 11935010 and 11775159), and the Natural Science Foundation of Shanghai (Grant Nos. 18ZR1442800 and 18JC1410900).)
*Corresponding authors. Email: wangchenyifang@gmail.com; Xonics@tongji.edu.cn
© 2021 Chinese Physical Society and IOP Publishing Ltd

the quantum heat transfer in the qubit-phonon hybrid system on an equal footing.

Moreover, the phononic logical operation requires smart phononic devices,[27] which efficiently manage thermal energy. In particular, negative differential thermal conductance (NDTC) is considered as the key functional component of the thermal transistor, which was initially proposed by Li *et al.* based on the classical phononic lattices.[27,38] Later, NDTC has also been extensively investigated in nonequilibrium quantum systems, spreading from metal-dielectric interfaces with nontrivial interface structure engineering,[39] nonequilibrium superconducting devices with tunable superconducting gap,[40,41] nonequilibrium impurity systems with Kondo effect,[42] to thermally driven spin Seebeck diodes and transistors.[43,44]

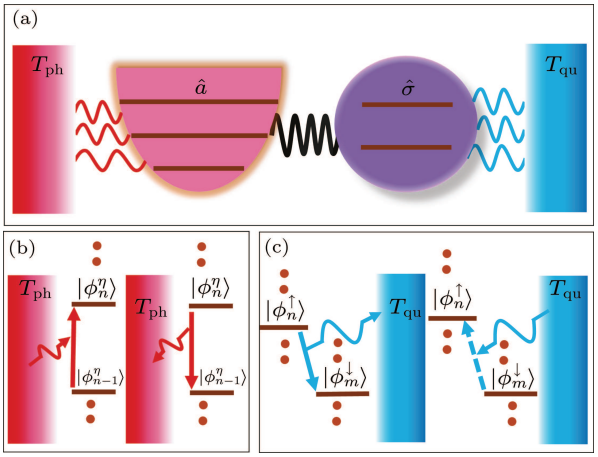

Fig. 1. (a) Schematic illustration of the single-mode phononic field (pink half-circle marked with $\hat{a}$) interacting with a two-level qubit (blue circle marked with $\hat{\sigma}$), each individually coupled to a thermal bath characterized as the temperature $T_{\rm ph}$ and $T_{\rm qu}$, with the dark wave line describing the interaction between the phonon mode and the qubit. (b) Transitions assisted by the ph-th bath are from $|\phi_{n-1}^\eta\rangle$ to $|\phi_n^\eta\rangle$ at Eq. (7a) and from $|\phi_n^\eta\rangle$ to $|\phi_{n-1}^\eta\rangle$ at Eq. (7b), with $\eta =\uparrow,\downarrow$ and $n\geq 1$. (c) Transitions assisted by the qu-th bath from $|\phi_n^\uparrow\rangle$ to $|\phi_m^\downarrow\rangle$ marked by the blue solid line, and transitions from $|\phi_m^\downarrow\rangle$ to $|\phi_n^\uparrow\rangle$ marked by the blue dashed line, which are both described by the rate expressions in Eqs. (8b) and (8a).

In this Letter, we investigate quantum heat transfer in the nonequilibrium qubit-phonon hybrid system in Fig. 1(a), which is one generic model of the phononic HQS. It should be noted that the qubit-phonon hybrid model is more than a toy model of theoretical interest. This hybrid system could be realized by the single quantum dot interacts with the nanomechanical resonator.[33,36] The nanomechanical resonator is driven by a thermal bath, and the quantum dot exchanges energy with a ferromagnetic insulator, which can be described as the bosonic (either phononic or magnonic) thermal bath.[43,44] The main points of this work have two folds: (i) We apply the dressed master equation embedded with coherent phonon state to study the steady state heat current of the qubit-phonon hybrid system, which is able to handle arbitrary qubit-phonon hybridization strengths. (ii) The NDTC is clearly exhibited with weak qubit-phonon interaction, whereas it disappears in strong qubit-phonon hybridization regime. The underlying microscopic mechanism is uncovered from the dynamical view.

The paper is organized as follows: Firstly, we introduce the qubit-phonon hybrid model, derive the quantum master equation combined with the coherent phonon states, and obtain the expression of steady state current. Secondly, we investigate the representative effects of thermal management, including NDTC, thermal rectification[45] and heat amplification.[38] The underlying mechanism of the NDTC and the connection among these effects are discussed. Finally, we give a brief summary.

Model and Method.—Nonequilibrium Qubit-Phonon Hybrid Model. The nonequilibrium qubit-phonon hybrid system typically consists of one qubit coupled to a single-mode phononic field, each interacting with an individual thermal bath, $\hat{H} = \hat{H}_{\rm s} + \sum_{u={\rm ph,qu}}(\hat{H}_u + \hat{V}_u)$, which is shown in Fig. 1(a). Specifically, the system Hamiltonian is expressed as[13]

$$\hat{H}_{\rm s} = \frac{\varepsilon}{2}\hat{\sigma}_z + \omega_0 \hat{a}^\dagger \hat{a} + \lambda \hat{\sigma}_z(\hat{a}^\dagger + \hat{a}), \tag{1}$$

where $\hat{\sigma}_z = |\uparrow\rangle\langle\uparrow| - |\downarrow\rangle\langle\downarrow|$ is the Pauli operator with the excited (ground) state $|\uparrow\rangle$ ($|\downarrow\rangle$) of the qubit, ε is the Zeeman splitting energy, $\hat{a}^\dagger$ ($\hat{a}$) creates (annihilates) one boson with the frequency ω_0, and λ is the interaction strength between the qubit and the bosonic field. Without loss of generality, we set $\omega_0 = 1$ as the energy unit throughout the whole work. The u-th bosonic thermal bath is described as $\hat{H}_u = \sum_k \omega_k \hat{b}_{k,u}^\dagger \hat{b}_{k,u}$, with $\hat{b}_{k,u}^\dagger$ ($\hat{b}_{k,u}$) creating (annihilating) one phonon (or magnon for $u = {\rm qu}$) with the frequency ω_k. The qu-th bath connects with the qubit, and the qubit-bath interaction is given by

$$\hat{V}_{\rm qu} = \hat{\sigma}_x \sum_k (f_{k,{\rm qu}} \hat{b}_{k,{\rm qu}}^\dagger + f_{k,{\rm qu}}^* \hat{b}_{k,{\rm qu}}). \tag{2}$$

The ph-th bath connects with the phononic field, and the phonon-bath interaction is given by

$$\hat{V}_{\rm ph} = (\hat{a}^\dagger + \hat{a}) \sum_k (f_{k,{\rm ph}} \hat{b}_{k,{\rm ph}}^\dagger + f_{k,{\rm ph}}^* \hat{b}_{k,{\rm ph}}), \tag{3}$$

with $\hat{\sigma}_x = |\uparrow\rangle\langle\downarrow| + |\downarrow\rangle\langle\uparrow|$ and $f_{k,{\rm qu(ph)}}$ the corresponding coupling strength. The u-th thermal bath is characterized as the spectral function $\gamma_u(\omega) = 2\pi \sum_k |f_{k,u}|^2 \delta(\omega - \omega_k)$, which is specified as the super-Ohmic form $\gamma_u(\omega) = \alpha_u \omega^3 \exp(-|\omega|/\omega_{c,u})/\omega_{c,u}^2$, with the coupling strength α_u and the cutoff frequency $\omega_{c,u}$.[46,47]

For the qubit-phonon interacting system described by Eq. (1), it can be exactly solved by applying the

coherent phonon states due to the commutating relation $[\hat{\sigma}_z, \hat{H}_{\rm s}] = 0$. Specifically, by projecting $\hat{H}_{\rm s}$ to the qubit states $|\uparrow\rangle$ and $|\downarrow\rangle$, we obtain $\hat{H}_{\rm s}|\uparrow\rangle = [\omega_0(\hat{a}^\dagger+\lambda/\omega_0)(\hat{a}+\lambda/\omega_0)-\lambda^2/\omega_0+\varepsilon/2]|\uparrow\rangle$ and $\hat{H}_{\rm s}|\downarrow\rangle = [\omega_0(\hat{a}^\dagger-\lambda/\omega_0)(\hat{a}-\lambda/\omega_0)-\lambda^2/\omega_0-\varepsilon/2]|\downarrow\rangle$. Hence, the eigenstates are given by $|\phi_n^\uparrow\rangle = |n\rangle_\uparrow \otimes |\uparrow\rangle$ and $|\phi_n^\downarrow\rangle = |n\rangle_\downarrow \otimes |\downarrow\rangle$, where the coherent phonon states are[33,48]

$$|n\rangle_\uparrow = \frac{(\hat{a}^\dagger+\lambda/\omega_0)^n}{\sqrt{n!}} \exp[-(\lambda/\omega_0)^2 - (\lambda/\omega_0)\hat{a}^\dagger]|0\rangle_a, \tag{4a}$$

$$|n\rangle_\downarrow = \frac{(\hat{a}^\dagger-\lambda/\omega_0)^n}{\sqrt{n!}} \exp[-(\lambda/\omega_0)^2 + (\lambda/\omega_0)\hat{a}^\dagger]|0\rangle_a, \tag{4b}$$

with the phononic Fock state in vacuum $\hat{a}|0\rangle_a = 0$. The corresponding eigenvalues are given by

$$E_{n,\uparrow} = \omega_0 n - \frac{\lambda^2}{\omega_0} + \frac{\varepsilon}{2}, \tag{5a}$$

$$E_{n,\downarrow} = \omega_0 n - \frac{\lambda^2}{\omega_0} - \frac{\varepsilon}{2}. \tag{5b}$$

Quantum Master Equation with Coherent Phonons. We apply the dressed quantum master equation combined with coherent phonon states to study steady state energy transfer behaviors of the qubit-phonon hybrid system, which can be validly applied from weak to strong qubit-phonon hybridization strengths.[49–52] Under the Born–Markov approximation, we consider weak system-bath interactions expressed by Eqs. (2) and (3). Then, the total density matrix is decomposed as $\hat{\rho}_{\rm tot}(t) \approx \hat{\rho}_{\rm s}(t) \otimes \hat{\rho}_b^{\rm ph} \otimes \hat{\rho}_b^{\rm qu}$, where $\hat{\rho}_{\rm s}(t)$ is the reduced density operator of the hybrid system and $\hat{\rho}_b^u = \exp(-\hat{H}_u/k_{\rm B}T_u)/{\rm Tr}\{\exp(-\hat{\rm H}_{\rm u}/{\rm k_B T_u})\}$ is the equilibrium distribution of the uth thermal bath, with $k_{\rm B}$ the Boltzmann constant and T_u the temperature of the uth thermal bath. By perturbing Eq. (2) and Eq. (3) in the eigenspace of $\hat{H}_{\rm s}$ up to the second order separately, we obtain the nonequilibrium dressed quantum master equation

$$\frac{d\hat{\rho}_{\rm s}}{dt} = -i[\hat{H}_{\rm s}, \hat{\rho}_{\rm s}] + \sum_{n,m;\eta,\eta';u} \{\Gamma_u^+(\phi_m^{\eta'}|\phi_n^\eta)\mathcal{D}[|\phi_n^\eta\rangle\langle\phi_m^{\eta'}|]\hat{\rho}_{\rm s} + \Gamma_u^-(\phi_m^{\eta'}|\phi_n^\eta)\mathcal{D}[|\phi_m^{\eta'}\rangle\langle\phi_n^\eta|]\hat{\rho}_{\rm s}\}, \tag{6}$$

where the dissipator is given by $\mathcal{D}[|\phi_m^{\eta'}\rangle\langle\phi_n^\eta|]\hat{\rho}_{\rm s} = |\phi_m^{\eta'}\rangle\langle\phi_n^\eta|\hat{\rho}_{\rm s}|\phi_n^\eta\rangle\langle\phi_m^{\eta'}| - \frac{1}{2}(|\phi_n^\eta\rangle\langle\phi_n^\eta|\hat{\rho}_{\rm s} + \hat{\rho}_{\rm s}|\phi_n^\eta\rangle\langle\phi_n^\eta|)$.

The non-zero transition rates involved with the phonon and the ph-th thermal bath are given by

$$\Gamma_{\rm ph}^+(\phi_n^\eta|\phi_{n+1}^\eta) = \gamma_{\rm ph}(\omega_0)n_{\rm ph}(\omega_0)(n+1), \tag{7a}$$

$$\Gamma_{\rm ph}^-(\phi_n^\eta|\phi_{n+1}^\eta) = \gamma_{\rm ph}(\omega_0)[1+n_{\rm ph}(\omega_0)](n+1), \tag{7b}$$

with the Bose–Einstein distribution function $n_{\rm ph}(\omega_0) = 1/[\exp(\omega_0/k_{\rm B}T_{\rm ph}) - 1]$, which are irrelevant with the qubit-phonon coupling strength. As shown in Fig. 1(b), $\Gamma_{\rm ph}^+(\phi_n^\eta|\phi_{n+1}^\eta)[\Gamma_{\rm ph}^-(\phi_n^\eta|\phi_{n+1}^\eta)]$ describes the transition from the coherent phonon state $|\phi_n^\eta\rangle(|\phi_{n+1}^\eta\rangle)$ to $|\phi_{n+1}^\eta\rangle(|\phi_n^\eta\rangle)$ by absorbing (releasing) one boson from (into) the ph-th thermal bath without qubit flip. They obey the detailed balance relationship $\Gamma_{\rm ph}^+(\phi_n^\eta|\phi_{n+1}^\eta)/\Gamma_{\rm ph}^-(\phi_n^\eta|\phi_{n+1}^\eta) = \exp(-\omega_0/k_{\rm B}T_{\rm ph}).\gamma_{\rm ph}(\omega)$ is the spectral function of the phononic bath, which is super-Ohmic as specified before.

While the non-zero transition rates involved with the qubit and the qu-th thermal bath are given by

$$\Gamma_{\rm qu}^+(\phi_m^{\bar{\eta}}|\phi_n^\eta) = \theta(\Delta_{m,\bar{\eta}}^{n,\eta})\gamma_{\rm qu}(\Delta_{m,\bar{\eta}}^{n,\eta})n_{\rm qu}(\Delta_{m,\bar{\eta}}^{n,\eta}) \cdot D_{nm}^2(2\lambda/\omega_0), \tag{8a}$$

$$\Gamma_{\rm qu}^-(\phi_m^{\bar{\eta}}|\phi_n^\eta) = \theta(\Delta_{m,\bar{\eta}}^{n,\eta})\gamma_{\rm qu}(\Delta_{m,\bar{\eta}}^{n,\eta})[1+n_{\rm qu}(\Delta_{m,\bar{\eta}}^{n,\eta})] \cdot D_{nm}^2(2\lambda/\omega_0), \tag{8b}$$

where the qubit state is $\bar{\eta} = \downarrow (\uparrow)$ for $\eta = \uparrow (\downarrow)$, the Heaviside function is $\theta(x) = 1$ for $x \geq 0$ and $\theta(x) = 0$ for $x < 0$, the energy gap is $\Delta_{m,\bar{\eta}}^{n,\eta} = E_{n,\eta} - E_{m,\bar{\eta}}$, the Bose–Einstein distribution function is $n_{\rm qu}(\omega) = 1/[\exp(\omega/k_{\rm B}T_{\rm qu})-1]$. Here $\gamma_{\rm qu}(\omega)$ is the spectral function of the qu-th bath composed of bosons (magnons), which is super-Ohmic as specified before. The coefficient $D_{nm}(2\lambda/\omega_0)$ originates from coherent phonon state overlap $D_{nm}(2\lambda/\omega_0) = (-1)^n{}_\uparrow\langle n|m\rangle_\downarrow$, which is specified as[33,48]

$$D_{nm}(x) = e^{-x^2/2} \sum_{l=0}^{\min[n,m]} \frac{(-1)^l\sqrt{n!m!}x^{n+m-2l}}{(n-l)!(m-l)!l!}. \tag{9}$$

As shown in Fig. 1(c), the rate $\Gamma_{\rm qu}^+(\phi_m^{\bar{\eta}}|\phi_n^\eta)$ describes the transition from the eigenstate $|\phi_m^{\bar{\eta}}\rangle$ to $|\phi_n^\eta\rangle$ by absorbing the energy quantum from the qu-th thermal bath, whereas $\Gamma_{\rm qu}^-(\phi_m^{\bar{\eta}}|\phi_n^\eta)$ describes the transition from $|\phi_n^\eta\rangle$ to $|\phi_m^{\bar{\eta}}\rangle$ by releasing the energy into the qu-th thermal bath. It strongly depends on the coupling strength characterized by the coefficient $D_{nm}(2\lambda/\omega_0)$. Such transitions would both change the coherent states of phonon and qubit encoded in the coherent phonon states, as shown in Eq. (4a).

Steady State Heat Current./ Under the temperature bias ($T_{\rm ph} \neq T_{\rm qu}$), a heat flow naturally occurs mediated by the qubit-phonon system at steady state. We apply the dressed quantum master equation (6) to obtain the population dynamics. Particularly, the evolution of the population $P_{n,\eta} = \langle\phi_n^\eta|\hat{\rho}_{\rm s}|\phi_n^\eta\rangle$ is given by

$$\frac{dP_{n,\eta}}{dt} = \sum_{u;m,\eta'} [\Gamma_u^+(\phi_m^{\eta'}|\phi_n^\eta)P_{m,\eta'} - \Gamma_u^+(\phi_n^\eta|\phi_m^{\eta'})P_{n,\eta}] + \sum_{u;m,\eta'} [\Gamma_u^-(\phi_n^\eta|\phi_m^{\eta'})P_{m,\eta'} - \Gamma_u^-(\phi_m^{\eta'}|\phi_n^\eta)P_{n,\eta}]. \tag{10}$$

By analyzing the state transitions in Eq. (10), the steady state heat current into the ph-th and qu-th thermal baths can be obtained as follows:

$$J_{\rm ph} = \sum_{n,\eta} \omega_0 [\Gamma^-_{\rm ph}(\phi^\eta_n|\phi^\eta_{n+1}) P^{\rm ss}_{n+1,\eta} - \Gamma^+_{\rm ph}(\phi^\eta_n|\phi^\eta_{n+1}) P^{\rm ss}_{n,\eta}], \tag{11a}$$

$$J_{\rm qu} = \sum_{n,m;\eta} \Delta^{n,\eta}_{m,\bar{\eta}} [\Gamma^-_{\rm qu}(\phi^{\bar{\eta}}_m|\phi^\eta_n) P^{\rm ss}_{n,\eta} - \Gamma^+_{\rm qu}(\phi^{\bar{\eta}}_m|\phi^\eta_n) P^{\rm ss}_{m,\bar{\eta}}]. \tag{11b}$$

The first (second) term in heat current $J_{\rm ph}$ describes the heat transfer into (out of) the ph-th bath via the energy down (up) transition from the state $|\phi^\eta_{n+1}\rangle$ ($|\phi^\eta_n\rangle$) to $|\phi^\eta_n\rangle$ ($|\phi^\eta_{n+1}\rangle$) by releasing (absorbing) energy ω_0. The first (second) term in heat current $J_{\rm qu}$ describes the heat transfer into (out of) the qu-th bath via the energy down (up) transition from the state $|\phi^\eta_n\rangle$ ($|\phi^{\bar{\eta}}_m\rangle$) to $|\phi^{\bar{\eta}}_m\rangle$ ($|\phi^\eta_n\rangle$) by releasing (absorbing) energy $\Delta^{n,\eta}_{m,\bar{\eta}}$. The steady state current $J_{\rm ss}$ from left to right is obtained as

$$J_{\rm ss} = J_{\rm qu} = -J_{\rm ph}, \tag{12}$$

where the energy conservation $J_{\rm ph}+J_{\rm qu}=0$ is fulfilled, and can be verified by Eqs. (10), (11a) and (11b).

In open quantum systems, when we study the transition between two eigenstates with the corresponding energy gap smaller than the system-bath coupling strength, the long-lived coherence contributed by the thermal bath induced indirect transitions, could significantly affect the transient and steady state behaviors in some open quantum systems.[53–57] Then, it will become problematic to use the secular approximation to study dissipative dynamics of open quantum systems.[53] However, in the nonequilibrium qubit-phonon hybrid system, there is no such indirect transitions assisted by the same bath between two near degenerate states. Specifically, two coherent phonon states for the ph-th bath induced transitions always have the same qubit state, i.e., no flip. It shows that the minimal energy gap is ω_0, which is much larger than the system-bath coupling strength. While for the qu-th bath, the state transition is simultaneously accompanied by the qubit flip. Hence, the indirect transition assisted by the qu-th bath only happens in the indirect way $|\phi^\eta_n\rangle \to |\phi^{\bar{\eta}}_m\rangle \to |\phi^\eta_k\rangle$. Accordingly, the energy gap between $|\phi^\eta_n\rangle$ and $|\phi^\eta_k\rangle$ far exceeds the system-bath interaction strength. Hence, the secular approximation considered in the dressed master equation (6) is valid in the present study.

Moreover, considering the direct population transition between two near degenerate states described by the population dynamics in Eq. (10), if the spectral function $\gamma_u(\omega)$ is quite small in the low frequency regime (e.g., Ohmic and super-Ohmic spectra with large ω_c), the transition between near degenerate states is difficult to make due to the weak contribution from the low frequency modes in thermal baths.[49–52] Hence, such direct transition should not be important in the steady state energy exchange process between the system and thermal baths. Here, since we use the super-Ohmic thermal baths in the dressed quantum master equation to study steady state heat transfer in the qubit-phonon hybrid system, the transition rate $\Gamma^\pm_{\rm qu}(\phi^\downarrow_{n+1}|\phi^\uparrow_n) \propto (\Delta^{n,\uparrow}_{n+1,\downarrow})^2$ becomes negligible between two states when they are near degenerate $\Delta^{n,\uparrow}_{n+1,\downarrow} \to 0$. As such, the off-diagonal elements of the reduced system density matrix are negligible at steady state. Therefore, we are sure that the dressed master equation is safely applicable in this work, where the steady state heat current is of primary interest.

Thermal management—Negative differential thermal conductance. NDTC is a typical nonlinear effect within the two-terminal setup,[38,58–60] where the heat flow $J_{\rm ss}$ is suppressed by increasing the temperature bias $\Delta T = T_{\rm ph} - T_{\rm qu}$. As is known, the concept of NDTC was initially proposed by B. Li and his colleagues.[27,38] Consequently, various novel mechanisms to exhibit NDTC in open quantum systems were demonstrated.[39–43] Here, we clearly demonstrate that in the nonequilibrium qubit-phonon model, NDTC can be exhibited at weak qubit-phonon hybridization and weak system-bath dissipation, whereas NDTC disappears in strong qubit-phonon hybridization regime. It should be noted that such result is valid both for the super-Ohmic and Ohmic thermal baths.

We investigate the NDTC by tuning qubit-phonon hybridization strength from weak to strong at resonance ($\varepsilon = \omega_0$) in Fig. 2(a). In the positive temperature bias regime ($\Delta T > 0$), it is interesting to find that with weak qubit-phonon coupling (e.g., $\lambda = 0.01$), the heat current shows linear increase with small ΔT; whereas it is monotonically suppressed with large temperature bias, and becomes nearly vanished as $\Delta T = 2$ (corresponding to $T_{\rm ph} = 2$ and $T_{\rm qu} = 0$). Hence, it clearly demonstrates the emergence of the NDTC. Accordingly, the qubit is frozen to the state $|\downarrow\rangle$ (i.e., $\langle\hat{\sigma}_z\rangle = -1$) in Fig. 2(b). In sharp contrast, such suppression feature of the heat current disappears in the strong qubit-phonon coupling regime (e.g., $\lambda = 0.4$). And the qubit population bias dramatically deviates from the -1. The existence of the NDTC is approximately limited to the coupling zone $\lambda \in (0, 0.1)$. While in the negative temperature bias regime ($\Delta T < 0$), the magnitude of heat current shows monotonic enhancement by increasing $|\Delta T|$, in absence of the signature of NDTC. Therefore, we conclude that NDTC can be exhibited by positively increasing the temperature bias between two thermal baths in the weak qubit-phonon interaction regime, similar to the behaviors in the NDTC of Fermi-spin-Boson hybrid systems, in

Refs. [39,43].

Next, we devote to understanding the NDTC effect at resonance with weak qubit-phonon interaction(e.g., λ=0.01). Accordingly, the coherent phonon state overlap coefficient at Eq. (9) is reduced to $D_{nm}(\frac{2\lambda}{\omega_0})\approx(-1)^n[\delta_{n,m}+\frac{2\lambda}{\omega_0}\sqrt{n+1}\delta_{n,m-1}-\frac{2\lambda}{\omega_0}\sqrt{n}\delta_{n,m+1}]$. The non-zero transition rates $\Gamma^{\pm}_{\rm qu}(\phi^{\eta'}_m|\phi^{\eta}_n)$ in Eqs. (8a) and (8b) are then approximated to

$$\Gamma^{\pm}_{\rm qu}(\phi^{\downarrow}_m|\phi^{\uparrow}_n)\approx\delta_{n,m}\kappa^{\pm}_{\rm qu}(\omega_0)+\delta_{n,m+1}\Big(\frac{2\lambda}{\omega_0}\Big)^2 n\kappa^{\pm}_{\rm qu}(2\omega_0), \quad (13a)$$

$$\Gamma^{\pm}_{\rm qu}(\phi^{\uparrow}_m|\phi^{\downarrow}_n)=0, \quad (13b)$$

where the sequential rates are

$$\kappa^{+}_{\rm qu}(\omega)=\theta(\omega)\gamma_{\rm qu}(\omega)n_{\rm qu}(\omega), \quad (14a)$$

$$\kappa^{-}_{\rm qu}(\omega)=\theta(\omega)\gamma_{\rm qu}(\omega)[1+n_{\rm qu}(\omega)]. \quad (14b)$$

At large temperature bias limit (e.g., $T_{\rm ph}\approx2$ and $T_{\rm qu}\approx0$), it is found that $\Gamma^{+}_{\rm qu}(\phi^{\downarrow}_m|\phi^{\uparrow}_n)=0$ and $\Gamma^{-}_{\rm qu}[\phi^{\downarrow}_{n(n-1)}|\phi^{\uparrow}_n]$ finite, which clearly demonstrate the unidirectional transfer from the dressed state $|\phi^{\uparrow}_n\rangle$ to $|\phi^{\downarrow}_{n(n-1)}\rangle$ assisted by the qu-th bath, illustrated by blue solid lines in Fig. 2(c). Meanwhile, the populations associated with spin-up are almost fully depleted at steady state, i.e. $P_{n,\uparrow}\approx0$, which explains $\langle\hat{\sigma}_z\rangle=-1$. This significantly blocks the energy transfer from the qubit to the qu-th bath. While the other branch of populations $P_{n,\downarrow}$ under the thermal equilibrium is distributed as $P^{\rm ss}_{n,\downarrow}\approx[1-e^{-\omega_0/(k_{\rm B}T_{\rm ph})}]e^{-n\omega_0/(k_{\rm B}T_{\rm ph})}$. Therefore, the steady state heat current $J_{\rm ss}$ nearly vanishes at large temperature bias, which leads to the emergence of NDTC.

As the qubit-phonon hybridization strength is beyond the weak coupling limit (e.g., $\lambda>0.1$), we can expand the coefficient $D_{nm}(2\lambda/\omega_0)$ up to the second order of λ/ω_0 as $D_{nm}(\frac{2\lambda}{\omega_0})\approx(-1)^n\{[1-(n+1/2)(\frac{2\lambda}{\omega_0})^2]\delta_{n,m}+\frac{2\lambda}{\omega_0}(\sqrt{n+1}\delta_{n,m-1}-\sqrt{n}\delta_{n,m+1})+\frac{1}{2}(\frac{2\lambda}{\omega_0})^2[\sqrt{n(n-1)}\delta_{n,m+2}+\sqrt{(n+1)(n+2)}\delta_{n,m-2}]\}$. Then, the transition rates are approximated as

$$\Gamma^{\pm}_{\rm qu}(\phi^{\downarrow}_m|\phi^{\uparrow}_n)\approx\delta_{n,m}\Big[1-(n+\frac{1}{2})(\frac{2\lambda}{\omega_0})^2\Big]^2\kappa^{\pm}_{\rm qu}(\omega_0)+\delta_{n,m+1}\Big(\frac{2\lambda}{\omega_0}\Big)^2 n\kappa^{\pm}_{\rm qu}(2\omega_0)+\delta_{n,m+2}\Big(\frac{2\lambda}{\omega_0}\Big)^4\frac{n(n-1)}{4}\kappa^{\pm}_{\rm qu}(3\omega_0), \quad (15a)$$

$$\Gamma^{\pm}_{\rm qu}(\phi^{\uparrow}_m|\phi^{\downarrow}_n)\approx\delta_{n,m+2}\Big(\frac{2\lambda}{\omega_0}\Big)^4\frac{n(n-1)}{4}\kappa^{\pm}_{\rm qu}(\omega_0). \quad (15b)$$

In particular, by increasing the temperature bias the relaxation transition from $|\phi^{\downarrow}_{n+2}\rangle$ to $|\phi^{\uparrow}_n\rangle$ [see the blue dashed line in Fig. 2(d) based on the non-zero rate $\Gamma^{-}_{\rm qu}(\phi^{\uparrow}_n|\phi^{\downarrow}_{n+2})$ at Eq. (15b)] should be necessarily included, which could keep $P_{n,\uparrow}$ finite, resulting in the excitation of the population bias ($\langle\hat{\sigma}_z\rangle>-1$) as shown in Fig. 2(b). Hence, this newly emerged relaxation rate $\Gamma^{-}_{\rm qu}(\phi^{\uparrow}_n|\phi^{\downarrow}_{n+2})$ helps to complete the thermodynamic cycle, which enables the finite energy transfer between the qubit and the qu-th bath. Therefore, it partially explains the suppression of the signature of NDTC beyond weak qubit-phonon interaction strength.

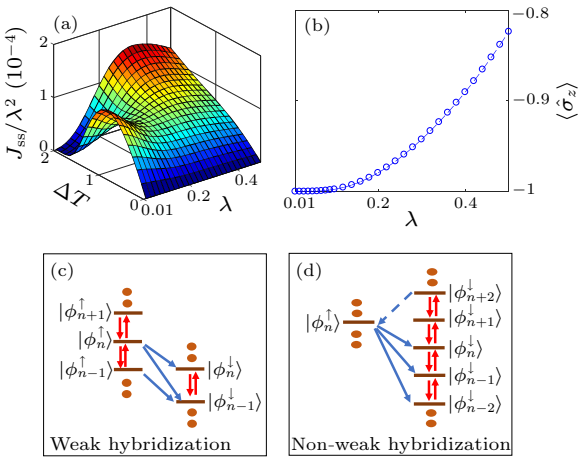

Fig. 2. (a) The bird-view of the heat current $J_{\rm ss}/\lambda^2$ by tuning both ΔT and λ, with $T_{\rm ph}=T_0+\Delta T/2$, $T_{\rm qu}=T_0-\Delta T/2$ and $T_0=1$; (b) The qubit population bias $\langle\hat{\sigma}_z\rangle$ as a function of λ at limiting temperature bias $\Delta T=2$; (c) Schematic illustration of eigenstate transitions at large temperature bias limit with weak qubit-phonon hybridization, where horizontal brown solid lines denote the eigenstate $|\phi^{\eta}_n\rangle$, up and down red solid lines with arrows represent transitions between eigenstates $|\phi^{\eta}_n\rangle$ and $|\phi^{\eta}_{n-1}\rangle$ at Eq. (7a) and Eq. (7b), the blue solid lines with arrows show transitions from $|\phi^{\uparrow}_n\rangle$ to $|\phi^{\downarrow}_n\rangle(|\phi^{\downarrow}_{n-1}\rangle)$ at Eq. (13a), and the transition from $|\phi^{\downarrow}_m\rangle$ to $|\phi^{\uparrow}_n\rangle$ is forbidden described at Eq. (13b). (d) Schematic illustration of eigenstate transitions beyond weak qubit-phonon hybridization, where the blue solid lines describe transitions from $|\phi^{\uparrow}_n\rangle$ to $|\phi^{\downarrow}_{n-m}\rangle$ with $m=0,1,2$ at Eq. (15a), and the blue dashed line describes the transition from $|\phi^{\downarrow}_{n+2}\rangle$ to $|\phi^{\uparrow}_n\rangle$ at Eq. (15b). Other parameters are given by $\omega_0=1$, $\varepsilon=1$, $\alpha_{\rm ph}=\alpha_{\rm qu}=0.005$, and $\omega_c=10$.

Moreover, we also analyze the effect of the energy bias $\delta=\omega_0-\varepsilon$ on the steady state heat current $J_{\rm ss}/\lambda^2$ with weak qubit-phonon interaction strength in Fig. 3(a). For discussion convenience we restrict $|\delta|<\omega_0$, which can be easily extended. It is found that by increasing the detuning δ from negative to positive, the current shows monotonic enhancement. While for NDTC, in the regime $\delta<0$ it always becomes significant, which results from the depletion of the populations $P_{n,\uparrow}\approx0$. However, in the regime $\delta>0$ the signature of NDTC gradually becomes suppressed with the increase of δ. From Eqs. (8a) and (8b), the transition rate assisted by the qu-th thermal bath is

approximated as

$$\Gamma^{\pm}_{\rm qu}(\phi^{\downarrow}_m|\phi^{\uparrow}_n)\approx\delta_{n,m}\kappa^{\pm}_{\rm qu}(\varepsilon)+\delta_{n,m-1}\left(\frac{2\lambda}{\omega_0}\right)^2 m\kappa^{\pm}_{\rm qu}(\varepsilon-\omega_0) + \delta_{n,m+1}\left(\frac{2\lambda}{\omega_0}\right)^2 n\kappa^{\pm}_{\rm qu}(\varepsilon+\omega_0), \quad (16a)$$

$$\Gamma^{\pm}_{\rm qu}(\phi^{\uparrow}_m|\phi^{\downarrow}_n)\approx\delta_{n,m-1}\left(\frac{2\lambda}{\omega_0}\right)^2 m\kappa^{\pm}_{\rm qu}(\omega_0-\varepsilon). \quad (16b)$$

It is known that $\delta<0$ always leads to $\kappa^{\pm}_{\rm qu}(\omega_0-\varepsilon)=0$. Hence, in the limiting temperature bias regime(e.g., $T_{\rm ph}\approx2$ and $T_{\rm qu}\approx0$), considering the energy exchange involved with the qu-th thermal bath, there only exist the unidirectional transitions from $|\phi^{\uparrow}_n\rangle\to|\phi^{\downarrow}_{n+k}\rangle$ ($k=0,\pm1$), which results in the persistence of NDTC. While as $\delta>0$, it is known that besides the unidirectional transitions $|\phi^{\uparrow}_n\rangle\to|\phi^{\downarrow}_n\rangle$ and $|\phi^{\uparrow}_n\rangle\to|\phi^{\downarrow}_{n-1}\rangle$, there exists the additional transition from $|\phi^{\downarrow}_{n+1}\rangle$ to $|\phi^{\uparrow}_n\rangle$ to avoids the populations $P_{n,\uparrow}$ from depletion, which is shown with the blue dashed line in Fig. 3(b). This mainly leads to the finite heat current and makes the NDTC suppressed.

It should be noted that the similar profile of NDTC can also be discovered at weak qubit-phonon hybridization and weak system-bath dissipation by replacing the super-Ohmic bath with the Ohmic bath, which is defined as $\gamma_u(\omega)=\alpha_u\omega\exp(-|\omega|/\omega_c)$. The main reason is that besides the nonzero rates shown by Eqs. (13a) and (13b) obtained from the general expression of the transitions rates in Eqs. (8a) and (8b), there could exist additional energy exchange process between two near degenerate eigenstates, e.g., $|\phi^{\uparrow}_{n-1}\rangle$ and $|\phi^{\downarrow}_n\rangle$ at resonance ($\omega_0=\varepsilon$), with nonzero transition rates $\Gamma^0_{\rm qu}(\phi^{\uparrow}_{n-1}|\phi^{\downarrow}_n)=8(\frac{\lambda}{\omega_0})^2 n\alpha_{\rm qu}k_{\rm B}T_{\rm qu}$. While in the large temperature bias limit (e.g., $T_{\rm ph}=2$ and $T_{\rm qu}=0$ given in Fig. 2), the rate $\Gamma^0_{\rm qu}(\phi^{\uparrow}_{n-1}|\phi^{\downarrow}_n)$ becomes negligible. Hence, the unidirectional transfer picture is identical with the counterpart in Fig. 2(c), which results in the appearance of NDTC naturally.

For the nonequilibrium spin-boson model, researchers applied the noninteracting blip approximation combined with the Marcus approximation, and reported NDTC at strong system-bath dissipation with Ohmic thermal baths.[61] However, it was later found that NDTC disappeared by applying the polaron-transformed Redfield equation without using the Marcus approximation,[62] which is completely identical to the noninteracting blip approximation as the spectral function of the thermal bath adopts the Ohmic case. Therefore, NDTC as an artifact of Marcus approximation does not exist in the nonequilibrium spin-Boson model with more rigorous treatments. It is also worth noting that by applying the reaction coordinate mapping approach, the nonequilibrium spin-boson model can be mapped to one special type of qubit-phonon hybrid systems. Hence, the exploration of the microscopic mechanism of NDTC in the qubit-phonon hybrid systems could fertilize the design of thermal operations beyond the spin-boson model.[61,62]

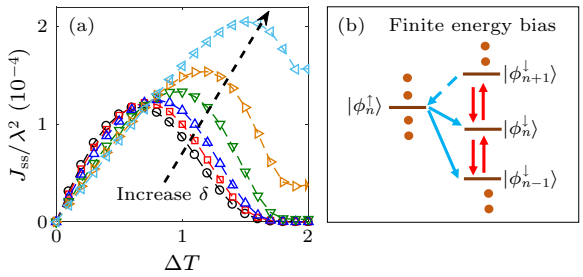

Fig. 3. (a) Effect of the qubit bias $\delta=\omega_0-\varepsilon$ (-0.8, -0.5, -0.2, 0.2, 0.5, 0.8 arrowed by the black dashed line) on the steady state heat current $J_{\rm ss}/\lambda^2$ at weak qubit-phonon coupling as a function of the temperature bias ΔT, with $T_{\rm ph}=T_0+\Delta T/2$, $T_{\rm qu}=T_0-\Delta T/2$, and $T_0=1$. (b) When $\delta>0$, the transitions from $|\phi^{\uparrow}_n\rangle$ to $|\phi^{\downarrow}_n\rangle$ and $|\phi^{\downarrow}_{n-1}\rangle$ (blue solid lines with arrow) in Eq. (16a), the transition from $|\phi^{\downarrow}_{n+1}\rangle$ to $|\phi^{\uparrow}_n\rangle$ (the blue dashed line with arrow) by Eq. (16b), and the transition between $|\phi^{\uparrow(\downarrow)}_n\rangle$ and $|\phi^{\uparrow(\downarrow)}_{n+1}\rangle$ (the red solid line with arrow) by Eqs. (7a) and (7b) in the large temperature bias regime ($\Delta T\approx2$). Other parameters are $\omega_0=1$, $\lambda=0.01$, $\alpha_{\rm ph}=\alpha_{\rm qu}=0.005$, and $\omega_c=10$.

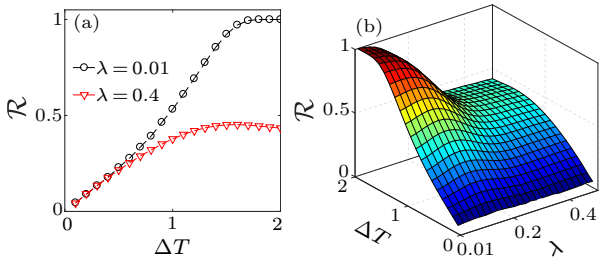

Fig. 4. Thermal rectification $\mathcal{R}$ (a) as a function of the temperature bias ΔT with $T_{\rm ph}=T_0+\Delta T/2$, $T_{\rm qu}=T_0-\Delta T/2$ and $T_0=1$, and (b) both modulating ΔT and the qubit-phonon coupling strength λ. The other parameters are $\omega_0=1$, $\varepsilon=1$, $\alpha_{\rm ph}=\alpha_{\rm qu}=0.005$, and $\omega_c=10$.

Thermal Rectification as a Quantum Heat Diode. Inspired by the asymmetric behavior of the heat current $J_{\rm ss}$ in Fig. 2(a), we investigate the thermal rectification effect by tuning temperature bias $\Delta T=T_{\rm ph}-T_{\rm qu}$ in Fig. 4. The thermal rectification is described as the behavior that the heat current in one direction is larger than the reversed heat current with the opposite bias.[27,46,63–67] The rectification factor is defined as[65,66]

$$\mathcal{R}=\frac{|J_{\rm ss}(\Delta T)+J_{\rm ss}(-\Delta T)|}{\max\{|J_{\rm ss}(\Delta T)|,|J_{\rm ss}(-\Delta T)|\}}, \quad (17)$$

where $J_{\rm ss}(\Delta T)$ represents the current with the temperatures $T_{\rm ph}=T_0+\Delta T/2$ and $T_{\rm qu}=T_0-\Delta T/2$. The thermal rectification becomes most significant as $\mathcal{R}=1$, and it vanishes when $\mathcal{R}=0$.[67] In Fig. 4(a), it is shown that the temperature bias generally enhances

the rectification factor at both weak and strong qubit-phonon couplings. In particular, the thermal rectification factor approaches unit with weak qubit-phonon interaction (e.g., $\lambda = 0.01$) and large temperature bias limit ($\Delta T \approx 2$), and is quite stable. Such perfect rectification becomes more apparent within the 3D view of $\mathcal{R}$ in Fig. 4(b).

While at strong qubit-phonon coupling, NDTC vanishes as described in Fig. 2(a), the finite rectification factor can still be observed. This mainly stems from the asymmetric structure of the qubit-phonon hybrid system,[64] similar to the Fermi-spin-Boson hybrid system.[39,43] Therefore, we conclude that the qubit-phonon hybrid system has the great potential to be a perfect thermal rectifier, and the significant thermal rectification favors weak qubit-phonon interaction.

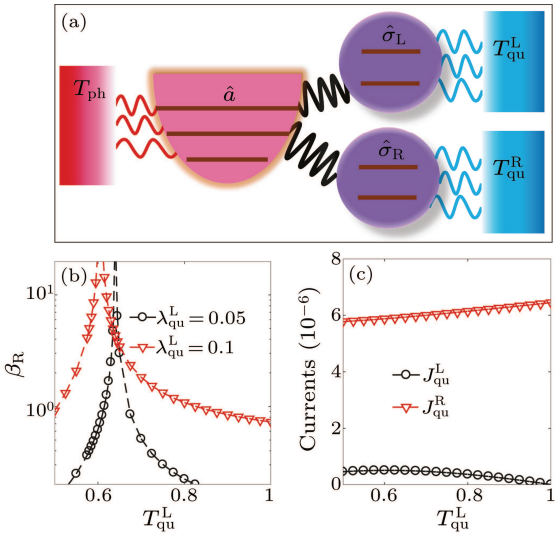

Fig. 5. (a) Schematic illustration of one phonon mode (pink half-circle marked as $\hat{a}$) coupled to two qubits [blue circles marked as $\hat{\sigma}_{L(R)}$], each individually interacting with a thermal bath characterized as the temperatures $T_{\rm ph}$, $T^{\rm L}_{\rm qu}$ and $T^{\rm R}_{\rm qu}$, respectively; (b) heat amplification factor $\beta_{\rm R}$ at Eq. (22) with left-qubit phonon coupling strength $\lambda^{\rm L}_{\rm qu} = 0.05, 0.1$, and (c) heat currents $J^{\rm L}_{\rm qu}$ and $J^{\rm R}_{\rm qu}$ at Eq. (11b) with $\lambda^{\rm L}_{\rm qu} = 0.1$ as a function of $T^{\rm L}_{\rm qu}$, both with right-qubit phonon coupling strength given by $\lambda^{\rm R}_{\rm qu} = 4\lambda^{\rm L}_{\rm qu}$. The other parameters are $\omega_0 = 1$, $\varepsilon = 1$, $\alpha_{\rm ph} = \alpha_{\rm qu} = 0.005$, $\omega_c = 10$, $T_{\rm ph} = 1.2$, and $T^{\rm R}_{\rm qu} = 0.2$.

Heat Amplification as a Quantum Thermal Transistor. The heat amplification effect is generally investigated within the three-terminal setup. We consider two qubits coupled to a phonon mode in Fig. 5(a), which is described as

$$\hat{H}_{\rm s} = \frac{1}{2}\sum_{v={\rm L,R}} \varepsilon_v \hat{\sigma}^v_z + \omega_0 \hat{a}^\dagger \hat{a} + \sum_{v={\rm L,R}} \lambda^v_{\rm qu} \hat{\sigma}^v_z (\hat{a}^\dagger + \hat{a}). \tag{18}$$

Based on the qubits basis $|\zeta\rangle$ with $\zeta = \eta_{\rm L}\eta_{\rm R}$ and $\eta_v = \{\uparrow, \downarrow\}$, the system Hamiltonian can be exactly solved as $\hat{H}_{\rm s}|\psi^\zeta_n\rangle = E^\zeta_n |\psi^\zeta_n\rangle$, where the eigenstate is given by the direct product of qubit states and coherent phonon states:

$$|\psi^\zeta_n\rangle = |\zeta\rangle \otimes \frac{(\hat{a}^\dagger + g_\zeta)^n}{\sqrt{n!}} \exp(-g^2_\zeta/2 - g_\zeta \hat{a}^\dagger)|0\rangle_a, \tag{19}$$

with the bare vacuum state $\hat{a}|0\rangle_a = 0$ and the displaced coefficients $g_{\uparrow\uparrow} = (\lambda^{\rm L}_{\rm qu} + \lambda^{\rm R}_{\rm qu})/\omega_0$, $g_{\uparrow\downarrow} = (\lambda^{\rm L}_{\rm qu} - \lambda^{\rm R}_{\rm qu})/\omega_0$, $g_{\downarrow\uparrow} = (-\lambda^{\rm L}_{\rm qu} + \lambda^{\rm R}_{\rm qu})/\omega_0$ and $g_{\downarrow\downarrow} = (-\lambda^{\rm L}_{\rm qu} - \lambda^{\rm R}_{\rm qu})/\omega_0$. The eigenvalue is $E^\eta_n = \omega_0 n + \Lambda_\eta$, with the displaced energies $\Lambda_{\uparrow\uparrow} = (\varepsilon_{\rm L} + \varepsilon_{\rm R})/2 - \omega_0 g^2_{\uparrow\uparrow}$, $\Lambda_{\uparrow\downarrow} = (\varepsilon_{\rm L} - \varepsilon_{\rm R})/2 - \omega_0 g^2_{\uparrow\downarrow}$, $\Lambda_{\downarrow\uparrow} = (-\varepsilon_{\rm L} + \varepsilon_{\rm R})/2 - \omega_0 g^2_{\downarrow\uparrow}$ and $\Lambda_{\downarrow\downarrow} = (-\varepsilon_{\rm L} - \varepsilon_{\rm R})/2 - \omega_0 g^2_{\downarrow\downarrow}$. Moreover, three thermal baths are given by $\hat{H}_b = \sum_{v=L,R,ph} \omega_k \hat{b}^\dagger_{k,v} \hat{b}_{k,v}$, and the system-bath interaction is given by $\hat{H}_{\rm sb} = \sum_{v,k}(f_{k,v}\hat{b}^\dagger_{k,v}\hat{S}_v + f^*_{k,v}\hat{b}_{k,v}\hat{S}^\dagger_v)$, with $\hat{S}_{L(R)} = \hat{\sigma}^{L(R)}_x$ and $\hat{S}_{\rm ph} = \hat{a}$. Then, by applying the similar dressed quantum master equation as shown in Eq. (6), we obtain the steady state currents into the ph-th and $L(R)$-th thermal baths $J_{\rm ph}$ and $J^{L(R)}_{\rm qu}$. Specifically, the expression of $J_{\rm ph}$ is similar to the counterpart in Eq. (11a) by only changing the qubits state index η with ζ, and $J^v_{\rm qu}$ is similarly given by

$$J^v_{\rm qu} = \sum_{n,m;\zeta} \Delta^{n,\zeta}_{m,\bar{\zeta}_v} [\Gamma^-_{{\rm qu},v}(\phi^{\bar{\zeta}_v}_m|\phi^\zeta_n) P^{\rm ss}_{n,\zeta} - \Gamma^+_{{\rm qu},v}(\phi^{\bar{\zeta}_v}_m|\phi^\zeta_n) P^{\rm ss}_{m,\bar{\zeta}_v}], \tag{20}$$

where $\bar{\zeta}_{\rm L} = \bar{\eta}_{\rm L}\eta_{\rm R}$ for $v = {\rm L}$ and $\bar{\zeta}_{\rm R} = \eta_{\rm L}\bar{\eta}_{\rm R}$ for $v = {\rm R}$ with $\bar{\eta}_v = \downarrow (\uparrow)$ for $\eta_v = \uparrow (\downarrow)$, the energy gap is $\Delta^{n,\zeta}_{m,\bar{\zeta}_v} = E^\zeta_n - E^{\bar{\zeta}_v}_m$, the transition rates are given by

$$\Gamma^+_{{\rm qu},v}\left(\phi^{\bar{\zeta}_v}_m|\phi^\zeta_n\right) = \theta\left(\Delta^{n,\zeta}_{m,\bar{\zeta}_v}\right)\gamma^v_{\rm qu}\left(\Delta^{n,\zeta}_{m,\bar{\zeta}_v}\right) n^v_{\rm qu}\left(\Delta^{n,\zeta}_{m,\bar{\zeta}_v}\right) \cdot D^2_{nm}(2\lambda^v_{\rm qu}/\omega_0), \tag{21a}$$

$$\Gamma^-_{{\rm qu},v}\left(\phi^{\bar{\zeta}_v}_m|\phi^\zeta_n\right) = \theta\left(\Delta^{n,\zeta}_{m,\bar{\zeta}_v}\right)\gamma^v_{\rm qu}\left(\Delta^{n,\zeta}_{m,\bar{\zeta}_v}\right) \cdot \left[1 + n^v_{\rm qu}\left(\Delta^{n,\zeta}_{m,\bar{\zeta}_v}\right)\right] \cdot D^2_{nm}(2\lambda^v_{\rm qu}/\omega_0), \tag{21b}$$

and the steady state population is $P^{\rm ss}_{n,\zeta} = \langle\psi^\zeta_n|\hat{\rho}_{\rm s}|\psi^\zeta_n\rangle$.

To analyze the heat amplification effect, we set the ph-th bath as the hot source, the R-th bath as the cold drain, and the L-th bath as the gate with the tunable temperature $T^{\rm L}_{\rm qu} \in [T^{\rm R}_{\rm qu}, T_{\rm ph}]$. The amplification factor is defined as[27]

$$\beta_{\rm R} = \left|\frac{\partial J^{\rm R}_{\rm qu}}{\partial J^{\rm L}_{\rm qu}}\right|. \tag{22}$$

The heat amplification occurs once the tiny change of $J^{\rm L}_{\rm qu}$ would dramatically modulate $J^{\rm R}_{\rm qu}$, specified as $\beta_{\rm R} > 1$. We focus on the heat amplification in the weak qubit-phonon coupling regime in Fig. 5(b), in which the NDTC generally appears as shown in Fig. 2. It is found that there exists a giant amplification factor in the moderate temperature regime (e.g., $T^{\rm L}_{\rm qu} \approx 0.6$ when $\lambda^{\rm L}_{\rm qu} = 0.1$). Accordingly, the heat current $J^{\rm L}_{\rm qu}$

is much smaller than $J_{\rm qu}^{\rm R}$ [see Fig. 5(c)], which ensures the valid application of this setup as a quantum thermal transistor. Moreover, the amplification becomes suppressed as the temperature $T_{\rm qu}^{\rm L}$ is tuned away from this giant factor regime. Then, it fails to realize the heat amplification in the small and large temperature limits of $T_{\rm qu}^{\rm L}$. Though not shown in this study, it should be noted that other setups can also realize the thermal transistor effect, e.g., exchanging the setup position of the qubit $\sigma_{\rm R}$ with the phonon mode a.

In summary, we have investigated quantum heat transfer and multifunctional thermal operations in the nonequilibrium qubit-phonon hybrid system, and applied the dressed quantum master equation combined with the coherent phonon states to study the steady state transport behaviors, which enables us to study the quantum heat flows with arbitrary qubit-phonon interaction strength. In particular, we have studied the effect of the temperature bias $\Delta T = T_{\rm ph} - T_{\rm qu}$ on the behavior of the steady state heat current. In the weak qubit-phonon coupling and finite temperature bias regime, it is found that the heat current shows dramatic decrease by increasing ΔT, which is a clear signature of NDTC. To unravel the underlying mechanism of NDTC, we have analyzed the transition processes from the dynamical view. It is found that the steady state populations corresponding to the qubit state $|\uparrow\rangle$ are depleted as $T_{\rm qu} \to 0$, which eliminates the energy exchange process between the qubit and the qu-th thermal bath. Moreover, we have investigated the influence of the qubit-phonon interaction on the phononic rectification and heat amplification. The perfect heat rectification ($\mathcal{R} = 1$) is observed with weak qubit-phonon coupling and large temperature bias, which corresponds to the significant NDTC. Meanwhile, the giant amplification factor is exhibited within the three-terminal setup.

We hope that the analysis of quantum heat transfer and thermal management in the qubit-phonon hybrid system have potential applications for efficient energy control and logical operations of phonon-based HQSs. We would like to point out that although the angular momentum conservation is not explicitly considered in the qubit-phonon hybrid system at present, it is implicitly contained in the phonon-qubit (spin) coupling, where the raising and lowering of the qubit's half spin will be compensated for by the creation and annihilation of phonons with ± 1 spin angular momentum.[68–70] Thus, quantum spin Seebeck transport[43] in such qubit-phonon hybrid systems is natural. Further investigation of the influence of quantum correlation on the energy transfer and energy management in the phononic HQSs should be intriguing to conduct in future.[24]

C. Wang would like to thank Jie-Qiao Liao for helpful discussion.

References

[1] Wallquist M, Hammerer K, Rabl P, Lukin M and Zoller P 2009 *Phys. Scr.* **T137** 014001
[2] Kurizki G, Bertet P, Kubo Y, Mølmer K, Petrosyan D, Rabl P and Schmiedmayer J 2015 *Proc. Natl. Acad. Sci. USA* **112** 3866
[3] Clerk A A, Lehnert K W, Bertet P, Petta J R and Nakamura Y 2020 *Nat. Phys.* **16** 257
[4] Blais A, Huang R S, Wallraff A, Girvin S M and Schoelkopf R J 2004 *Phys. Rev. A* **69** 062320
[5] Wallraff A, Schuster D I, Blais A, Frunzio L, Huang R S, Majer J, Kumar S, Girvin S M and Schoelkopf R J 2004 *Nature* **431** 162
[6] Niemczyk T, Deppe F, Huebl H, Menzel E P, Hocke F, Schwarz M J, Garcia-Ripoll J J, Zueco D, Hummer T, Solano E, Marx A and Gross R 2010 *Nat. Phys.* **6** 772
[7] O'Connell A D, Hofheinz M, Ansmann M, Bialczak R C, Lennander M, Lucero E, Neeley M, Sank D, Wang H, Weides M, Wenner J, Martinis J M and Cleland A N 2010 *Nature* **464** 697
[8] You J Q and Nori F 2011 *Nature* **474** 589
[9] Zhou L, Yang L P, Li Y and Sun C P 2013 *Phys. Rev. Lett.* **111** 103604
[10] Acevedo O L, Quiroga L, Rodríguez F J and Johnson N F 2015 *New J. Phys.* **17** 093005
[11] Cirac J I, Zoller P, Kimble H J and Mabuchi H 1997 *Phys. Rev. Lett.* **78** 3221
[12] Kimble H J 2008 *Nature* **453** 1023
[13] Rabl P, Kolkowitz S J, Koppens F H L, Harris J G E, Zoller P and Lukin M D 2010 *Nat. Phys.* **6** 602
[14] Kolkowitz S, Jayich A C B, Unterreithmeier Q P, Bennett S D, Rabi P, Harris J G E and Lukin M D 2012 *Science* **335** 1603
[15] Yeo I, de Assis P L, Gloppe A, Dupont-Ferrier E, Verlot P, Malik N S, Dupuy E, Claudon J, Gerard J M, Auffeves A, Nogues G, Seidelin S, Poizat J P, Arcizet O and Richard M 2014 *Nat. Nanotechnol.* **9** 106
[16] Schuetz M J A, Kessler E M, Giedke G, Vandersypen L M K, Lukin M D and Cirac J I 2015 *Phys. Rev. X* **5** 031031
[17] Bienfait A, Satzinger K J, Zhong Y P, Chang H S, Chou M H, Conner C R, Dumur E, Grebel J, Peairs G A, Povey R G and Cleland A N 2019 *Science* **364** 368
[18] Pechal M, Arrangoiz-Arriola P and Safavi-Naeini A H 2018 *Quantum Sci. Technol.* **4** 015006
[19] Hann C T, Zou C L, Zhang Y X, Chu Y W, Schoelkopf R J, Girvin S M and Jiang L 2019 *Phys. Rev. Lett.* **123** 250501
[20] Ceban V, Longo P and Macovei M A 2017 *Phys. Rev. A* **95** 023806
[21] Droenner L, Naumann N L, Kabuss J and Carmele A 2017 *Phys. Rev. A* **96** 043805
[22] Montenegro V, Coto R, Eremeev V and Orszag M 2018 *Phys. Rev. A* **98** 053837
[23] Maguire H, lles-Smith J and Nazir A 2019 *Phys. Rev. Lett.* **123** 093601
[24] Micadei K, Peterson J P S, Souza A M, Sarthour R S, Oliveira I S, Landi G T, Batalhao T B, Serra R M and Lutz E 2019 *Nat. Commun.* **10** 2456
[25] Man Z X, Zhang Q and Xia Y J 2019 *Quantum Inf. Process.* **18** 157
[26] Latune C L, Sinayskiy I and Petruccione F 2019 *Phys. Rev. Res.* **1** 033097
[27] Li N B, Ren J, Wang L, Zhang G, Hanggi P and Li B 2012 *Rev. Mod. Phys.* **84** 1045
[28] He D H, Thingna J, Wang J S and Li B 2016 *Phys. Rev. B* **94** 155411

[29] Zhang Z Q and Lü J T 2017 *Phys. Rev. B* **96** 125432
[30] He D H, Thingna J and Cao J S 2018 *Phys. Rev. B* **97** 195437
[31] Zhu J X and Balatsky A V 2003 *Phys. Rev. B* **67** 165326
[32] Zippilli S, Morigi G and Bachtold A 2009 *Phys. Rev. Lett.* **102** 096804
[33] Ren J, Zhu J X, Gubernatis J E, Wang C and Li B 2012 *Phys. Rev. B* **85** 155443
[34] Arrachea L, Bode N and von Oppen F 2014 *Phys. Rev. B* **90** 125450
[35] Stadler P, Belzig W and Rastelli G 2014 *Phys. Rev. Lett.* **113** 047201
[36] Stadler P, Belzig W and Rastelli G 2016 *Phys. Rev. Lett.* **117** 197202
[37] Härtle R, Schinabeck C, Kulkarni M, Gelbwaser-Klimovsky D, Thoss M and Peskin U 2018 *Phys. Rev. B* **98** 081404
[38] Li B, Wang L and Casati G 2006 *Appl. Phys. Lett.* **88** 143501
[39] Ren J and Zhu J X 2013 *Phys. Rev. B* **87** 241412(R)
[40] Ren J and Zhu J X 2013 *Phys. Rev. B* **87** 165121
[41] Fornieri A, Timossi G, Bosisio R, Solinas P and Giazotto F 2016 *Phys. Rev. B* **93** 134508
[42] Sierra M A, López R and Lim J S 2018 *Phys. Rev. Lett.* **121** 096801
[43] Ren J 2013 *Phys. Rev. B* **88** 220406(R)
[44] Ren J and Zhu J X 2013 *Phys. Rev. B* **88** 094427
[45] Li B, Wang L and Casati G 2004 *Phys. Rev. Lett.* **93** 184301
[46] Leggett A J, Chakravarty S, Dorsey A T, Fisher M P A, Garg A and Zwerger W 1987 *Rev. Mod. Phys.* **59** 1
[47] Weiss U 2008 *Quantum Dissipative Systems* (Singapore: World Scientific)
[48] Chen Q H, Zhang Y Y, Liu T and Wang K L 2008 *Phys. Rev. A* **78** 051801
[49] Beaudoin F, Gambetta J M and Blais A 2011 *Phys. Rev. A* **84** 043832
[50] Ridolfo A, Leib M, Savasta S and Hartmann M J 2012 *Phys. Rev. Lett.* **109** 193602
[51] Ridolfo A, Savasta S and Hartmann M J 2013 *Phys. Rev. Lett.* **110** 163601
[52] Boite A L, Hwang M J, Nha H C and Plenio M B 2016 *Phys. Rev. A* **94** 033827
[53] Tscherbul T V and Brumer P 2014 *Phys. Rev. Lett.* **113** 113601
[54] Li S W, Cai C Y and Sun C P 2015 *Ann. Phys.* **360** 19
[55] Eastham P R, Kirton P, Cammack H M, Lovett B W and Keeling J 2016 *Phys. Rev. A* **94** 012110
[56] Wang C, Xu D Z, Liu H and Gao X L 2019 *Phys. Rev. E* **99** 042102
[57] Wang Z H, Wu W and Wang J 2019 *Phys. Rev. A* **99** 042320
[58] He D H, Buyukdagli S and Hu B 2009 *Phys. Rev. B* **80** 104302
[59] He D H, Ai B Q, Chan H K and Hu B 2010 *Phys. Rev. E* **81** 041131
[60] Chan H K, He D H and Hu B 2014 *Phys. Rev. E* **89** 052126
[61] Segal D 2006 *Phys. Rev. B* **73** 205415
[62] Wang C, Ren J and Cao J S 2015 *Sci. Rep.* **5** 11878
[63] Ruokola T, Ojanen T and Jauho A P 2009 *Phys. Rev. B* **79** 144306
[64] Ojanen T 2009 *Phys. Rev. B* **80** 180301
[65] Zhang L F, Yan Y H, Wu C Q, Wang J S and Li B W 2009 *Phys. Rev. B* **80** 172301
[66] Zhang L F, Wang J S and Li B W 2010 *Phys. Rev. B* **81** 100301
[67] Balachandra V, Pereira E, Casati G and Poletti D 2018 *Phys. Rev. Lett.* **120** 200603
[68] Long Y, Ren J and Chen H 2018 *Proc. Natl. Acad. Sci. USA* **115** 9951
[69] Shi C *et al.* 2019 *Natl. Sci. Rev.* **6** 707
[70] Long Y, Zhang D, Yang C, Ge J, Chen H and Ren J 2020 *Nat. Commun.* **11** 4716